

LEONID 1998 TRACKING CAMPAIGN AND DATA ANALYSIS

EXECUTIVE SUMMARY

Executive Summary of
ESA/ESOC Contract No. 13121/98/D/IM

ESA/ESOC Technical Supervisor: R. Jehn

The work described in this report was done under ESA/ESOC contract. Responsibility for the contents resides in the authors or organisations that prepared it.

April 2000

LEONID 1998 TRACKING CAMPAIGN AND DATA ANALYSIS

Observations of the 1998 Leonids were made by Electro-optical instruments in Mongolia and Australia, multi-frequency radar observations in Australia and global visual observations by amateur observers. These results have been used in conjunction with numerical modelling of the stream to address major issues of stream formation and evolution as well as specific aspects of the 1998 shower.

The major results which have been found for the 1998 Leonids are:

Two material components have been clearly identified in 1998. They include:

(1) A component of large meteoroids occurring approximately 20 hours before the time of nodal passage through the orbit of 55P/Tempel-Tuttle. Visual and video observations show a clear non-exponential number distribution at large masses, with an inflection point near absolute magnitude +2. Larger meteoroids show a more steep distribution, making them a larger overall fraction of the total observed population on the night of Nov 16, 1998. Modelling has identified these meteoroids with ejecta of order 500 – 1000 years of age, but not tied to any one specific ejection epoch (i.e. they are dust sheets composed of material of many different ages within this range).

(2) A second component, richer in small meteoroids showing a dual-peaked character in visual and video observations. These maxima correspond to the timing expected of the “traditional” maximum near the nodal passage time of the parent comet. Two peaks in the flux make up the traditional peak – one near 18 UT on 17 November, 1998 and a second peak near 21 UT on 17 November. These are best defined in the global visual flux data (see Appendix A), but they are also noticeable as a “dip” in the flux at video masses. Modelling of this component shows clear evidence that the early sub-maxima (near 18 UT) is associated with material released in 1932 and the later one (near 21 UT) with material ejected in 1965 (see Appendix B).

Electro-optical instruments in Mongolia have provided our best estimates for Leonid meteoroid flux and mass distributions in the mass range 10^{-7} – 10^{-5} kg. Additionally, analysis of the light curves of Leonids recorded from Mongolia have provided better estimates for the physical structure of individual Leonid meteoroids. In particular, from a sample of 1509 total Leonids recorded from Nov 16-17-18, 1998, However, for the mass range covered by these

image intensified cameras the peak flux occurred during the interval 19.5 UT to 22 UT on Nov 17 1998, within uncertainty of the time of predicted maximum. The peak is not well defined, and is rather broad at these faint magnitudes. Peak fluxes with the wide field of view cameras indicate that approximately 0.01 Leonids of mass greater than 4×10^{-8} kg would strike a one square kilometer surface (perpendicular to the shower radiant) per hour at the peak of the 1998 shower. At least three different cameras show a distinct dip in the flux between 20 and 21 UT on Nov. 17. This is possibly a hint of two populations within the 1998 Leonid shower, an observation supported by flux information gathered at larger masses from detailed global observations (see Annex A). The final electro-optical report presents more detailed time-profiles of the flux of Leonids at TV masses in 1998.

For comparison, the statistically weak radar echo fluxes from all three radar systems produced an estimated peak flux near 0.02 Leonids per square kilometre per hour with masses greater than 10^{-8} kg at the time of the peak (20 – 21 UT 17 Nov, 1998). No shape is evident in the flux profile due to the low number of Leonid echoes which were recorded.

TV data yields a mass distribution index value of $s=1.52 \pm 0.09$, in good agreement with visual and other video data from that night. This compares with a value of $s=1.71$ from the peak night on the 1997 Leonid data, indicating the richness of this year's shower in bright meteors. There is some hint of a change in slope for the brighter meteors on 16 November, which is confirmed by more robust statistics from global magnitude distributions. The radar mass index was found to be even lower, near $s=1.4$, but little weight is placed on this measurement due to the small number of echoes involved on 17 November.

Two major outstanding questions regarding the physical structure of Leonid meteoroids have been addressed by the TV measurements in 1998. First, the makeup of these fast meteoroids is probed sensitively by the beginning height of ablation. There is a strong linkage between the degree of volatility in the meteoroids and the altitude of their beginning heights. From the single station results we have 188 Leonid meteors which have their apparent beginning luminosity within the field of view. The majority of these Leonid meteors (66.0%) have beginning heights between 100 and 130 km. However, there are 14.9% which have heights in excess of 145 km (versus 10.1% with beginning heights below 100 km). If this height distribution is real, then the tail of high Leonid beginning heights are indicative of some very volatile luminous component in the meteors, or an extremely porous structure.

In contrast, video observations from two-stations are much more limited in number than the single station, but the precision of the heights (typically less than 2 km on individual heights) is much better. The double station results do not confirm the high Leonid beginning height tail from the single station results. For example, if one uses first appearance heights (not necessarily beginning heights) the double station results had only 5.7% in excess of 130 km and none in excess of 145 km. More than 88% of the sample was in the range from 100 to 130 km. It is not clear whether the difference between the two height distributions is because the double station results are biased to a common height by the need of coincidence detection within both fields of view, or if the high Leonid tail in the single station results is simply a consequence of the errors inherent in the single station technique, particularly for fast meteors with few video frames. The true nature of the height distribution at small sizes is a major outstanding issue which directly impacts on the volatile makeup of the Leonid meteoroids.

The second outstanding physical question associated with the Leonids is the nature of their physical structure. Precise heights and light curves were obtained for 77 Leonids recorded from two stations which ranged in brightness (at maximum luminosity) from +0.3 to +6.1 astronomical magnitude. The mean photometric mass of the data sample was 1.4×10^{-6} kg. The height distribution, combined with numerical modelling of the ablation of the meteoroids, suggests that silicate-like materials are not the principle component of Leonid meteoroids, and hints at the presence of a more volatile component. Light curves of many Leonids were examined for evidence of the physical structure of the associated meteoroids: like the 1997 Leonids, the sharp, nearly symmetric curves imply that the meteoroids are not solid objects. The light curves are consistent with a dustball structure. This dustball structure, in conjunction with the approximate physical character of the volatile fraction in the meteoroids, combines to form a picture of Leonid meteoroids as fluffy, dustball aggregates held together by a low temperature volatile “glue”, potentially organic in origin.

Modelling of the long-term behaviour of the Leonid stream has demonstrated that storms from the shower are from meteoroids less than a century in age and are due to trails from Tempel-Tuttle coming within $(8 \pm 6) \times 10^{-4}$ A.U of the Earth’s orbit on average. Trails are perturbed to Earth-intersection through distant, direct perturbations, primarily from Jupiter. The stream decreases in flux by two to three orders of magnitude in the first hundred years of development. Ejection velocities are found to be < 20 m/s and average ~ 5 m/s for storm meteoroids. Jupiter controls evolution of the stream after a century; radiation pressure and initial

ejection velocities are significant factors only on shorter time-scales. The age of the annual component of the stream is ~1000 years.

A detailed application of this model to the 1998 Leonids is given in Appendix B.

Appendix A: Detailed Visual Observations of the 1998 Leonid Shower

Summary

A detailed activity profile for the 1998 Leonid shower has been generated from global visual observations. The shower showed at least two distinct components - a broad component peaking between $234.^{\circ}4$ - $235.^{\circ}0$ and two narrower filaments near $235.^{\circ}21$ and $235.^{\circ}33$ of younger origin. This dual-peaked structure in the flux profile had peak fluxes to a limiting magnitude of +6.5 of 0.03 Leonids $\text{km}^{-2} \text{hour}^{-1}$. The distribution of particles also changes dramatically across the stream in 1998 with large meteoroids dominating the early peak and smaller meteoroids relatively more abundant near the time of the nodal passage of the comet.

Introduction

Here we present detailed visual results of the 1998 shower with emphasis on the sub-structures visible in the flux and particle distribution profiles. The visual observations consist of some 70800 Leonids recorded by 473 observers in 43 countries during the period November 3 - 29, 1998. Total effective observing time for this study was 2171 hours. The source for all visual data was the Visual Meteor Database (VMDB) maintained by the International Meteor Organization (IMO) (cf. Arlt, 1999).

Visual Results

Magnitude distributions

The methods used to collect and analyze visual data follow the standards established by the IMO (see Rendtel et al. (1995) for a detailed description). For the present study only Leonid magnitude distributions are selected for the determination of population indices r which fulfill three criteria: At least five consecutive magnitude classes should be involved in the resulting r -value. The faintest of these magnitude classes should be more than two magnitudes from the stellar limiting magnitude. This constraint results from the increased uncertainty in correction factors near the limiting magnitude. The probability of detecting a meteor is extremely low near the limiting magnitude, and small meteor numbers seen by the observer will be corrected to very

large true meteor numbers, thus introducing large errors. The total number of meteors in the magnitude distribution should be equal to or larger than 20. This figure has been found empirically to be the minimum useful for a single measure of the population index. The true number of meteors in each magnitude class (i.e. meteor number seen corrected with the perception probability) is larger than 3.0. The perception probabilities have been taken from meteors recorded in "double-count" observations, where two observers face fixed parts of the sky and note the relative positions of meteors. Figure 1 shows the population index profile between November 16, 1800 UT and November 18, 0050 UT. There are three local maxima visible in this graph : the first during the fireball peak near $234.^{\circ}67 \pm 0.^{\circ}05$, another just before the nodal peak at $\lambda=235.^{\circ}18 \pm 0.^{\circ}04$ and the most distinct local maxima close to the nodal passage of 55P/Tempel-Tuttle at $\lambda=235.^{\circ}34 \pm 0.^{\circ}01$. Here the population index r , refers to the ratio $N(M+1)/N(M)$, where M is the meteor magnitude and $N(M)$ the true number of meteors recorded in the M^{th} magnitude interval.

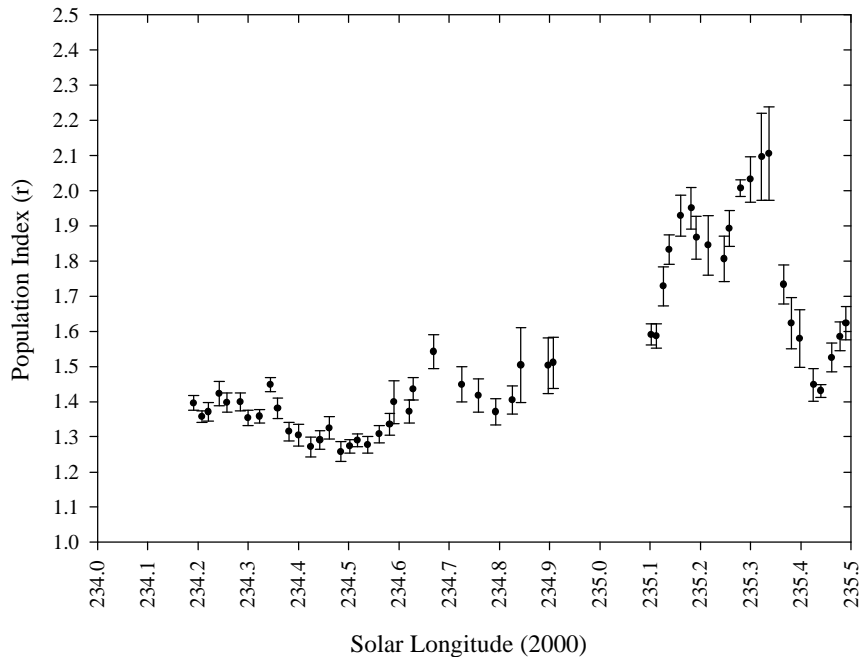


Figure 1 High-resolution profile of the population index r of the 1998 Leonids covering the period of highest activity.

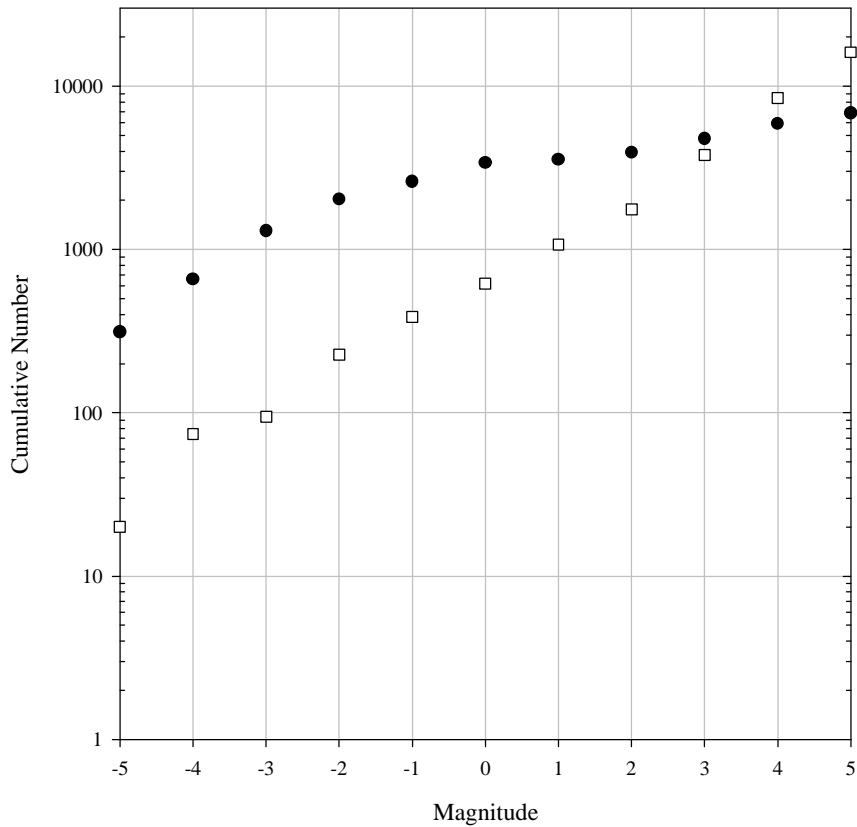


Figure 2 Cumulative magnitude distribution for all Leonids recorded between $\lambda=234.^{\circ}0-235.^{\circ}0$ (filled circles) and from $\lambda=235.^{\circ}0-235.^{\circ}5$ (open squares).

The calculation of the population index assumes that the cumulative number of shower meteors versus the magnitude follows an exponential distribution characterized by a single exponent. In fact, an exponential distribution delivers the same linear slope ($\log r$ for cumulative and non-cumulative distributions if the number of meteors is large). Figure 3 shows the logarithmic cumulative magnitude distribution for Leonids in the interval of the fireball maximum (solid circles) and the regular maximum near the nodal passage of 55P/Tempel-Tuttle (open squares) for all observations with limiting magnitudes of +6.0 or better. Note that the observed numbers of Leonids have been corrected for the perception probability in each magnitude class (cf. Rendtel et al., 1995). The former distribution is clearly not a single exponential distribution over the entire magnitude range shown - specific r values derived over this interval are not quantitatively meaningful. During the fireball maximum the particle mass

distribution appears to deviate from an exponential for equivalent magnitudes brighter than +2. The enhancement in moderately bright Leonids (near -2 to -3) is more than an order of magnitude greater as compared to the period near the nodal maximum (where $r \sim 1.8$ fits the distribution well over the entire magnitude range).

The ZHR profile

The first step in computing the Zenithal Hourly Rate (ZHR) is determining the population index profile as was done above. Observers' shower meteor numbers are then corrected according to their stellar limiting magnitudes to the standard magnitude of +6.5. The high-resolution graph of Figure 2 might reflect possible spurious, statistical variations onto the ZHR profile; we therefore applied a coarser population index profile for the computation of the ZHR. The window size for this smooth r -profile was $0.^\circ 2$ shifted by $0.^\circ 1$. Two selection criteria were applied to all individual ZHR values before they were to be used in the final averages:

1. Minimum radiant elevation of 20°
2. Maximum correction factor of $r^{(6.5-lm)}F/\sin h$ is less than 5, where lm is the stellar limiting magnitude, F is a factor for possible obstructions of the field of view, and h is the radiant elevation.

The ZHR profile for the entire period of significant activity of the Leonids in 1998 is given in Figure 3. The ZHR profile during the time of the fireball "maximum" is shown in Fig. 4 while that near the nodal maximum is shown in Fig. 5. In 1998, the ZHR maximum occurs at $\lambda=234.^\circ 53 \pm 0.^\circ 01$ with a magnitude of 357 ± 11 . From Figure 4 it is evident that a significant number of additional sub-maxima in the ZHR profile occur in the region of the fireball peak, most notably near $\lambda=234.^\circ 28$, $\lambda=234.^\circ 4$, $\lambda=234.^\circ 48$, $\lambda=234.^\circ 62$, $\lambda=234.^\circ 7$ and $\lambda=234.^\circ 81$. However, when the number of observers contributing data in each interval is examined, it becomes clear that some of these peaks may be observational artifacts. In particular, we note that a minima (with less than 15 observers contributing) in the number of observers used per interval are found in the regions near $\lambda=234.^\circ 28$, $\lambda=234.^\circ 38$, $\lambda=234.^\circ 46$, $\lambda=234.^\circ 62$, $\lambda=234.^\circ 71$ and at $\lambda=234.^\circ 78$. The correlation of these observer minima with the ZHR maxima casts doubt on the significance of some of these features as the relative paucity of observers in these solar longitude

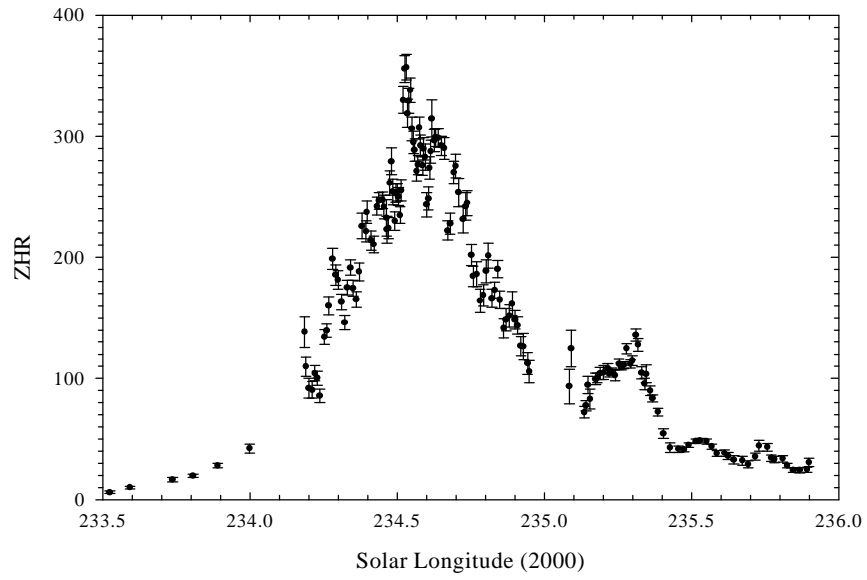


Figure 3. The ZHR profile of the 1998 Leonids from $\lambda=233.^{\circ}5-236.^{\circ}0$.

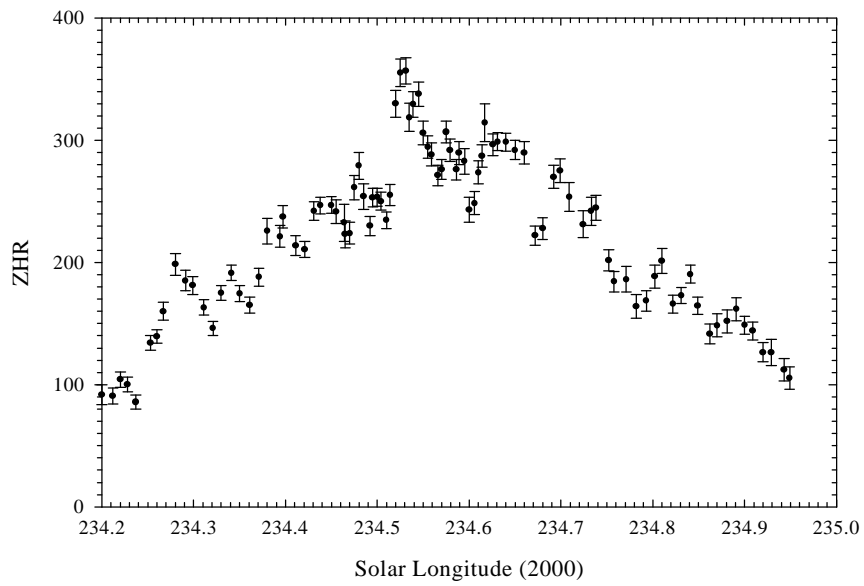


Figure 4. ZHR profile of the 1998 Leonids centred about the fireball peak.

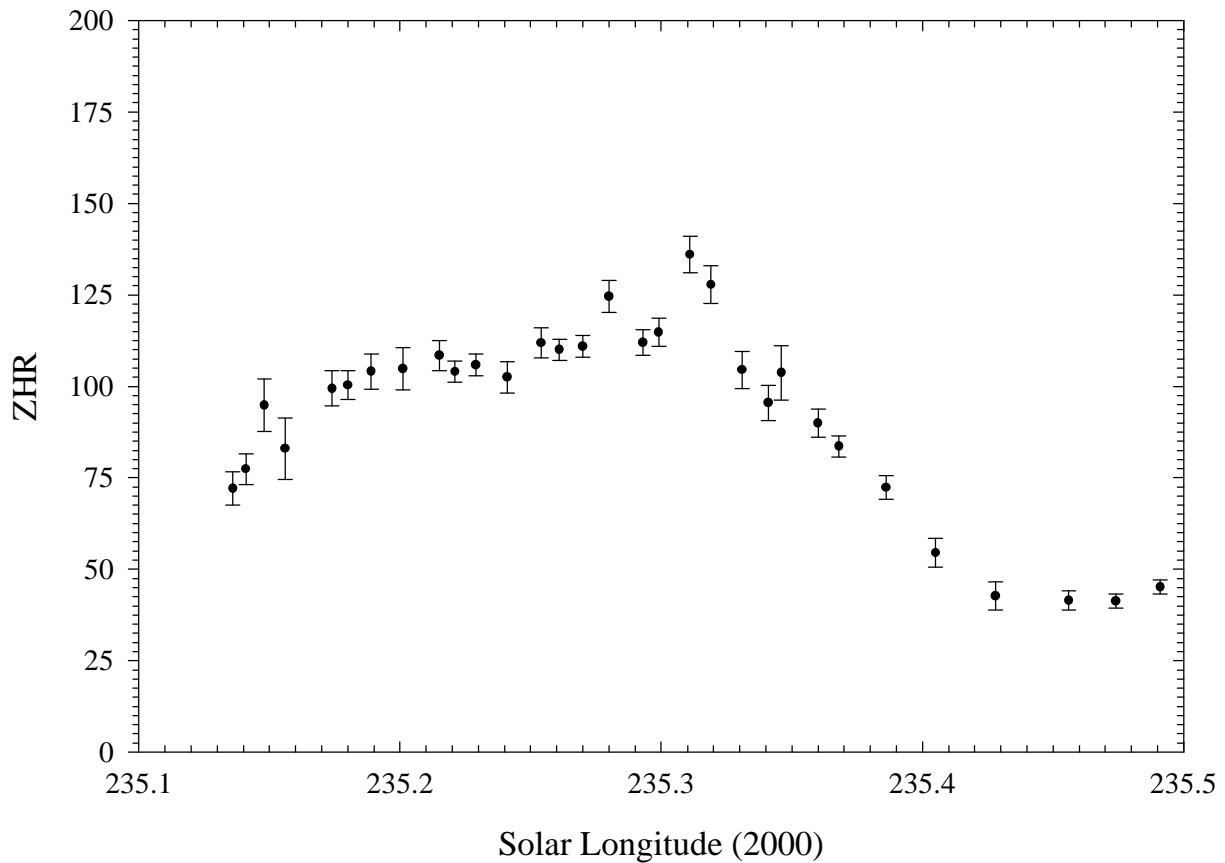


Figure 5. ZHR profile of the 1998 Leonids centred about the nodal peak.

intervals may produce a small systematic increase in the ZHR relative to neighboring intervals. The overall full-width to half-maximum for the fireball peak is found to be in the range 11-13 hours; this duration corresponds to a thickness for this stream component perpendicular to the orbital plane of approximately 400 000 km. The period near the nodal maximum is shown in Figure 5 with the location of the peak at $\lambda=234.^{\circ}31 \pm 0.^{\circ}01$ with a magnitude of 136 ± 5 . Comparing the location of this maximum to the r profile in Figure 1 we find that the location of maximum coincides almost directly with the maximum in the population index, with a difference of 40 minutes between the times of the two maxima. The ZHR profile is best described as flat from $\lambda=235.^{\circ}3-235.^{\circ}3$ with a near constant value of 100-110

The Flux

By using the population index and ZHR measures together, we are able to derive an absolute influx of Leonids above a specified magnitude threshold. Details for calculation of flux are given in Brown and Rendtel (1996) and Arlt (1998). As the fireball peak and nodal peak have dramatically different particle populations, we show flux calculated at three differing absolute magnitude levels. Figure 6 shows the flux at three different magnitude thresholds. The top is for very bright Leonids ($M_{V_{abs}} > -4$ or mass > 1 g), the middle for medium visual brightness Leonids ($M_{V_{abs}} > +3$ or mass $> 10^{-3}$ g) and the bottom panel for Leonids with $M_{V_{abs}} > +6.5$ or mass $> 2 \times 10^{-5}$ g. As expected, the fireball maximum completely dominates the flux at the largest masses, while extension to the smallest masses makes the nodal peak dominant.

Heuristically this can be understood from the fact that the effective collecting area in the atmosphere for visual observers is much larger for brighter meteors (as during the night of the fireball peak) and this is what causes the integrated flux at the smallest masses to be modest at the time of the fireball maximum (in contrast to the much smaller collecting areas during the nodal peak when r was higher). Most notable is the pronounced double maximum near the time of the nodal peak at the smallest masses, a feature not typically found in other shower profiles (see Rendtel et al. 1995). Figure 7 shows the flux in this solar longitude range in greater detail. The first maximum occurs at $\lambda = 235.^\circ 21 \pm 0.^\circ 02$ and is followed by a pronounced minimum occurring at $\lambda = 235.^\circ 26 \pm 0.^\circ 01$, the present nodal position of 55P/Tempel-Tuttle. The second maximum occurs at $\lambda = 235.^\circ 33 \pm 0.^\circ 01$. It is probable that this structure is the direct result of the change in the population index (see Figure 1) across this solar longitude range and hints directly at two different (recent) ejection origins for these two maxima.

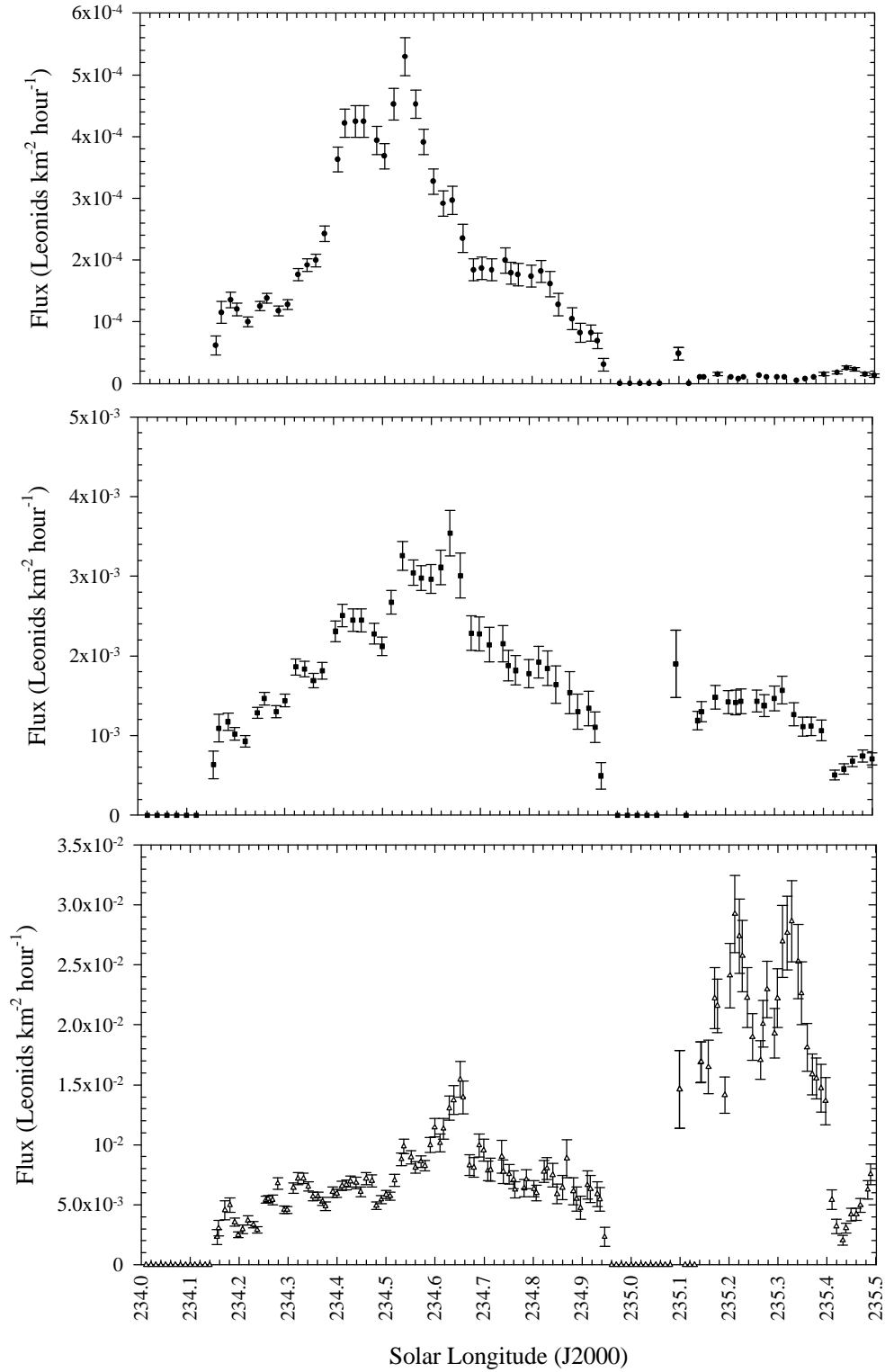


Figure 6. The flux profile of the Leonids at three threshold sizes. For Leonids with $M_{\text{Vabs}} > -4$ (top), $M_{\text{Vabs}} > +3$ (middle) and $M_{\text{Vabs}} > +6.5$ (bottom)

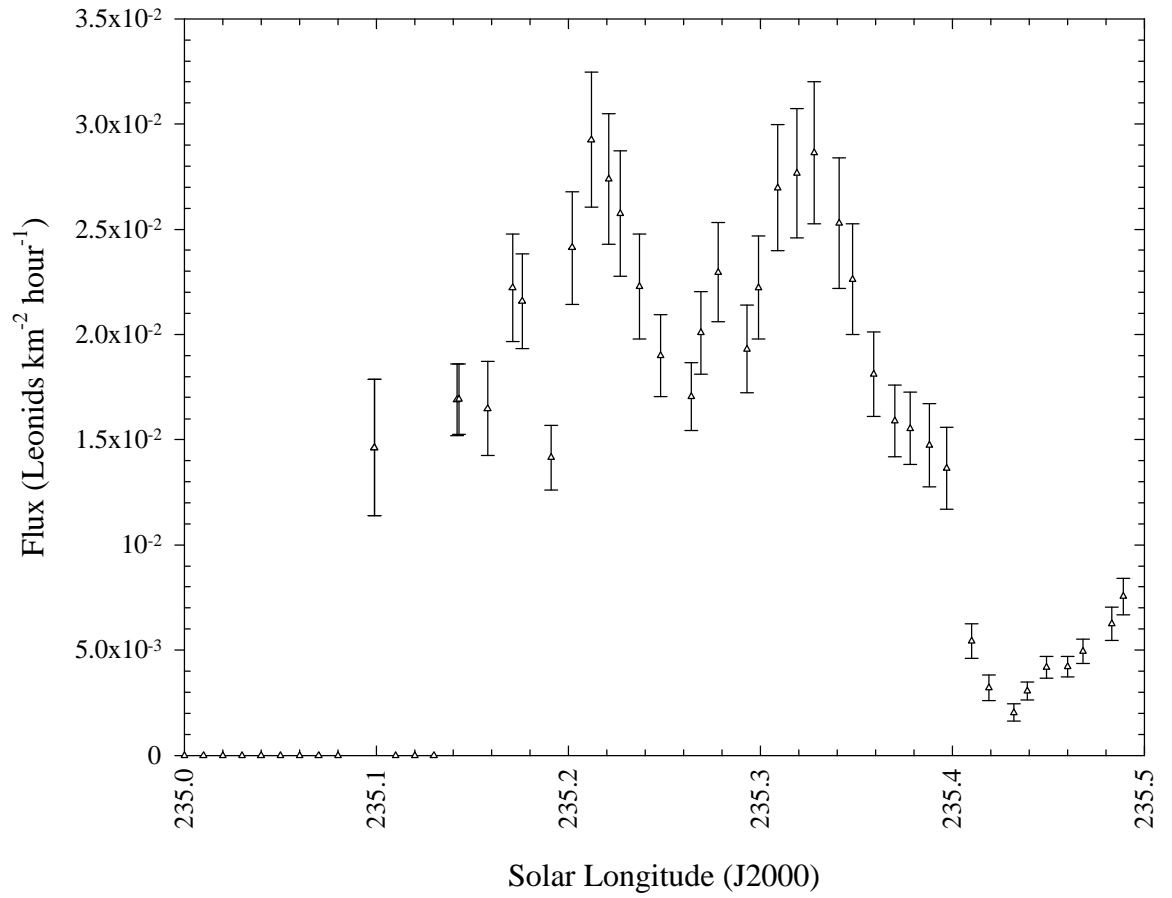


Figure 7. The flux profile of the Leonids near the time of the nodal maximum for Leonids with $M_{Vabs} > +6.5$.

Appendix B: Application of the Numerical Model to the 1998 Leonid Shower

Overview of model

To examine the Leonid material encountered by the Earth in 1998, we have used the output of a numerical model which consists of generating a suite of test particles close to each perihelion passage of Tempel-Tuttle and following each of these through to the epoch of interest. "daughter" Leonids are created through random ejection on the sunward hemisphere of Tempel-Tuttle and are distributed at random in true anomaly inside 4 A.U. The osculating elements for 55P/Tempel-Tuttle are taken from Yeomans et al. (1996). A total of 10 000 test meteoroids are ejected in each decadal mass interval from $10 \text{ g} - 10^{-5} \text{ g}$, for a total per perihelion passage of 70 000 test particles. This procedure is repeated for each of the last 15 perihelion passages of the comet so that each complete "run" consists of almost 1 million test particles. In addition to these 500 year-long "runs", a single run spanning 2000 years was performed for one model to examine effects of older ejections on the 1998 shower. For the 2000-year run (composed of 57 perihelion passages), the ejection velocities are given by the modified Whipple formula (cf. Brown and Jones, 1998).

After the initial conditions are specified in this way, each test particle is numerically integrated forward from ejection to the epoch of interest and followed until it reaches its descending node (the only point along its orbit at which it might possibly be observable from the Earth) and its Keplerian elements at the time of nodal passage are stored. The integration includes the direct and indirect perturbations of all planets from Venus to Neptune, radiation pressure and the Poynting-Robertson effect. The integrator used is a 4th order variable step-size Runge-Kutta (Jones, 1985). This basic procedure is repeated for four different physical models of ejection and three different values of meteoroid bulk density for a total of 12 different runs. The four physical models are derived from the work of Crifo (1995) on distributed gas production within the cometary coma and the Jones (1995) model with variations in the heliocentric dependence on ejection velocity and a parabolic distribution in meteoroid ejection probabilities. For each of these models we adopt bulk meteoroid densities of 0.1, 0.8 and 4.0 g cm^{-3} in turn, due

to uncertainties in the actual meteoroid bulk density and to investigate the role of differing assumed densities on the evolution of the stream. These densities, along with the range in initial particle masses, translate into a range of β 's from 10^{-5} - 10^{-2} . Our approach is to generate initial conditions which are "reasonable" within the constraints of our imperfect understanding of the cometary coma dust environment rather than to suggest any particular model as most appropriate. In particular, we recognize there to be large uncertainties in many of the physical quantities (i.e. density of meteoroids, relationship between meteoroid mass and luminosity etc.) and choose instead to explore the effects of widely different (but still "reasonable") ejection conditions (velocities, points of ejection and ejection directions) and meteoroid densities over a wide range of masses in this Monte Carlo fashion. This same approach has been used previously to study the formation and evolution of the Perseid stream (Brown and Jones, 1998) and more extensive details and discussion can be found in that work. Our hope is to identify effects insensitive to initial conditions and thus likely to be true features of the stream.

Results for 1998

All material ejected with nodal passages times within one week of the shower in 1998 were classified as possible Leonids. The nodal distances for each "streamlet" from all models ejected since 1633 are shown in Figure 1; the mean nodal distance from the sun for all particles and the standard deviation of the population are also given. Note that we have summed over all solar longitudes and for all masses from 10^{-3} g and larger for all models to produce this graph. The size of the standard deviation gives a first-order estimate of the sunward extension of each streamlet per model. As can be seen from the small difference between each model, the choice of initial ejection velocity distributions has a minor influence over the radial extent of streamlet. The location of all these recently produced streamlets in 1998 was considerably sunward of Earth, typically by distances of 0.005 - 0.008 A.U. The fact that none of the standard deviations of any model for any streamlet back to 1633 overlaps the Earth suggests that few particles from these ejection epochs would be expected to encounter Earth in 1998, as was observed. In fact, examination of the output from all models shows no significant numbers of Leonids intersecting the Earth back to the longest (500 year) model runs. Examination of the

longer (2000 year) runs, however, reveals a population dominated by larger meteoroids originating from ejections in the 500 - 1000 year old range and forming the parent population which produced the fireball peak in 1998 and we examine these data next.

The fireball peak

To examine the model output for the 1998 Leonid fireball peak, we limit our selection of test particles further to only those occurring in the solar longitude interval from $\lambda=234.^{\circ}0-235.^{\circ}0$. Figure 2 shows the number of test particles which were within one week of nodal passage at the time of the Earth's nodal crossing of Tempel-Tuttle's orbit in 1998 as well as being spatially within 0.001 A.U. of Earth's orbit for all perihelion passages since 79 A.D. Noteable is that little recent (less than 500 year old) material is present and that the meteoroids appear to originate in ejections which are 500 - 1000 years old. We note that no one ejection epoch completely dominates the delivery of material over this solar longitude interval in 1998. We also remark that all the model runs extending back only 500 years show only small numbers of test particles accepted in 1998, and these are all from the oldest ejections included in those runs. As a result, we confine the remainder of our examination of the fireball peak to the 2000 year-old run. Figure 3 shows the distribution by mass as a function of solar longitude for particles accepted in the interval of the fireball peak. It is clear that very large Leonids are preferentially associated with this solar longitude interval and (from Figure 2) that these derive from many perihelion passages of Tempel-Tuttle during the 12th-14th century. Figure 4 shows the distribution of accepted Leonids as a function of solar longitude and nodal distance. Note that several epochs have many large Leonids contributing to 1998 which originate from ejection near perihelion. It should also be emphasized that the ejection velocity interval sampled here is limited the Whipple ejection equation - in particular, the ejection velocities near perihelion are generally above $\sim 10\text{ms}^{-1}$.

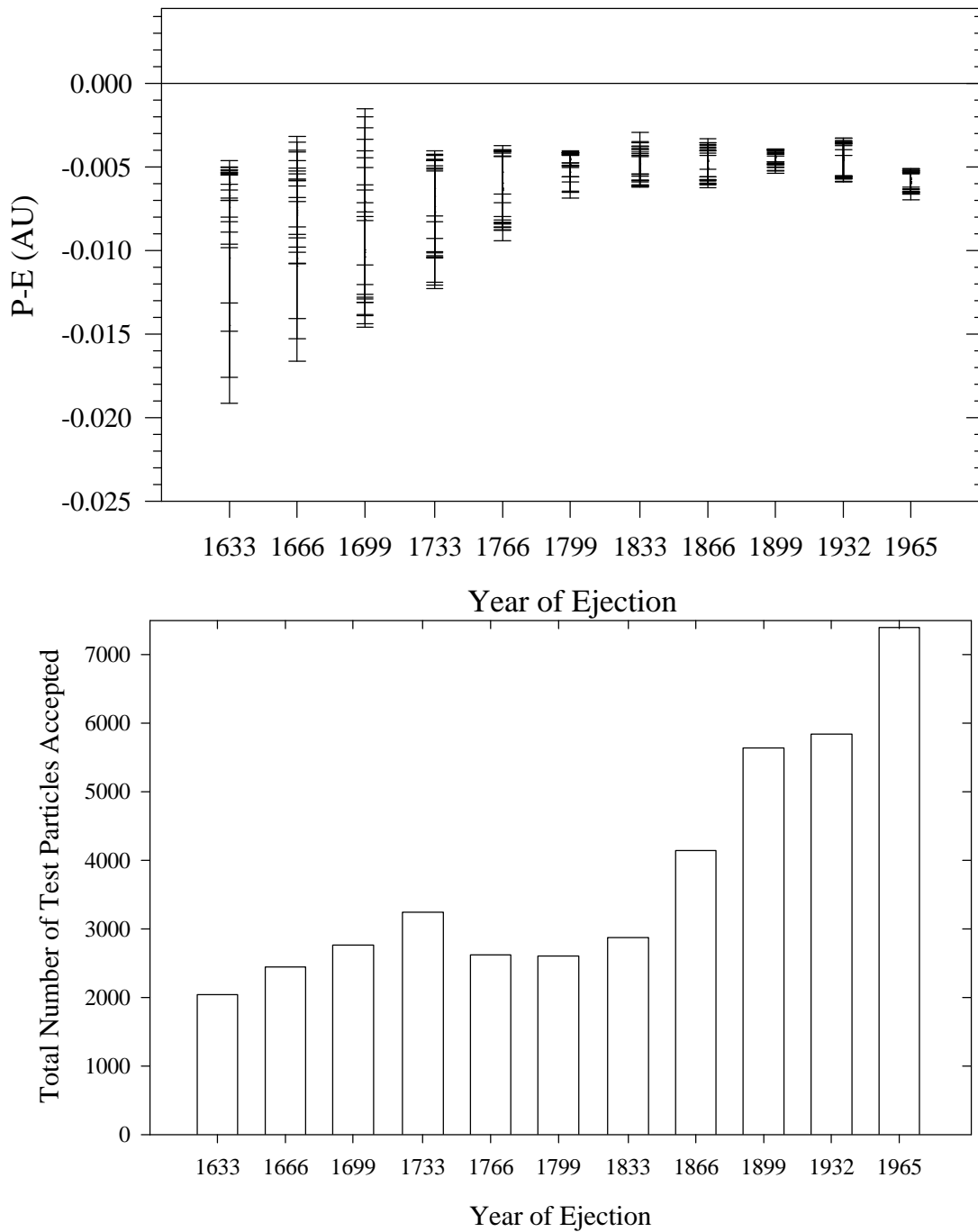


Figure 1. Distribution of nodal distances for test particles with mass=10g from several ejection eras (see Figure legend) as a function of solar longitude (top). Total number of accepted test particles per perihelion passage (bottom)

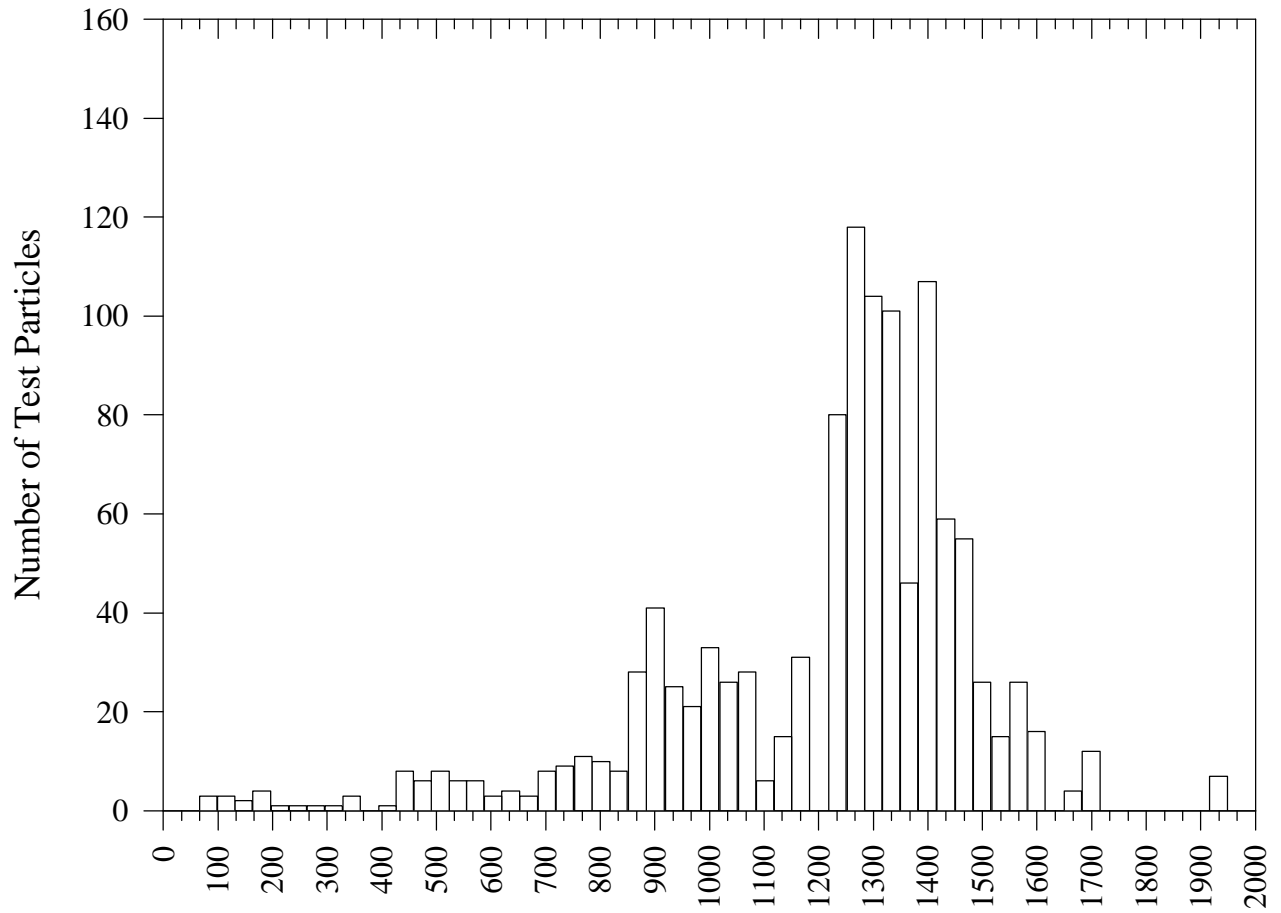


Figure 2. Number of test particles for 1998 Leonids per perihelion passage for meteoroids with $m > 10^{-3}$

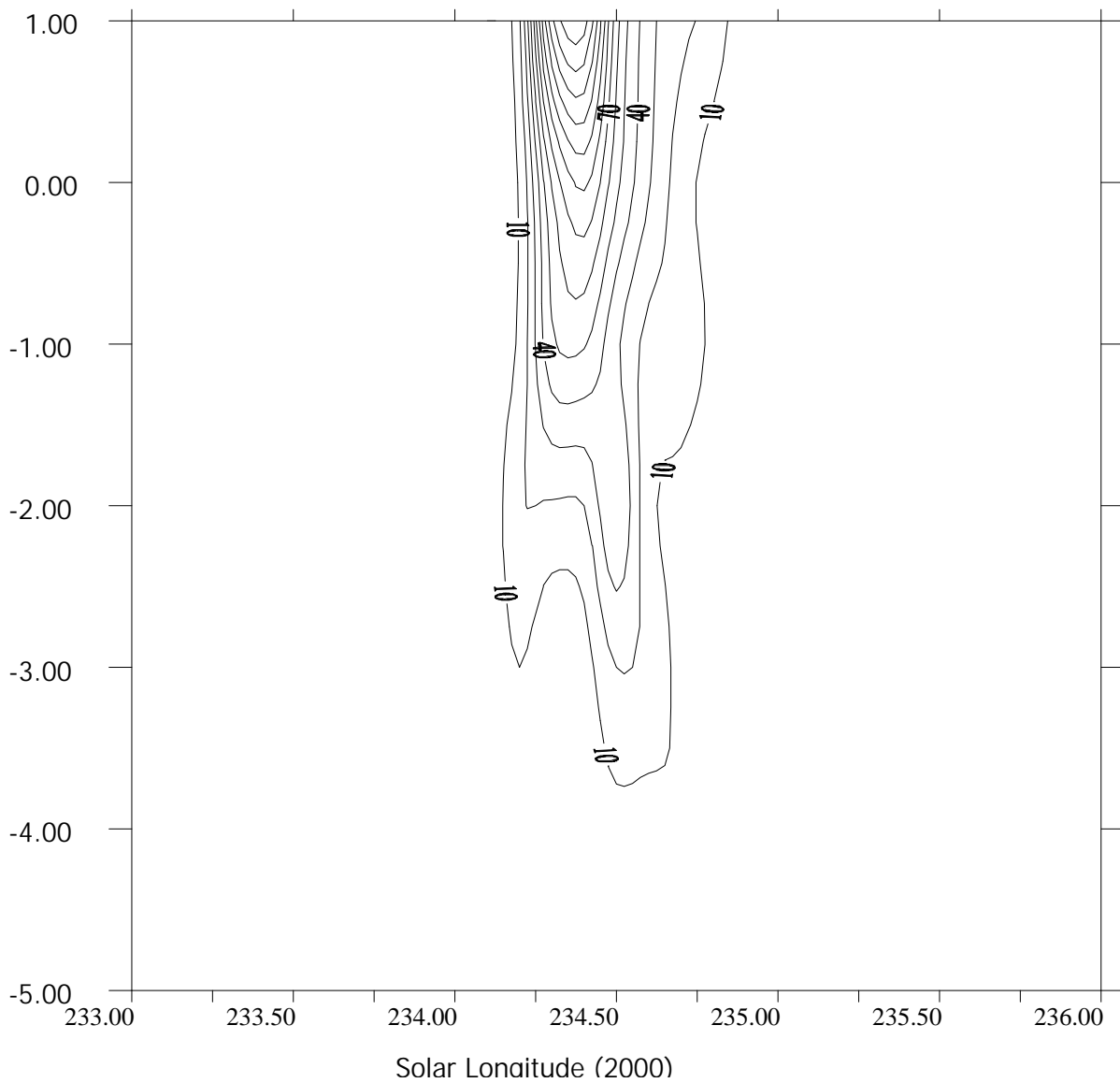


Figure 3. The 1998 Leonid test particles by mass as a function of solar longitude for ejections over the last 2000 years.

The nodal peak

From Figure 3 it is apparent that few particles of recent ejection origin with $\beta < 10^{-3}$ come close to Earth's orbit in 1998 using the ejection conditions adopted for the 2000-year modelling. In particular, the three most recent ejections have most material well inside the Earth's orbit, with large numbers of meteoroids concentrated more than 0.003 A.U. away from Earth's orbit. Of particular interest for the origin of the nodal peak, are the three most recent ejections with particles concentrated in the solar longitude interval near $\lambda = 235.^\circ 2 - 235.^\circ 4$. Almost all ejection models used here (with total ejection velocities

over 100 ms^{-1} for the smallest particles) produced very little material within 0.001 A.U. of Earth at the time of the shower in 1998.

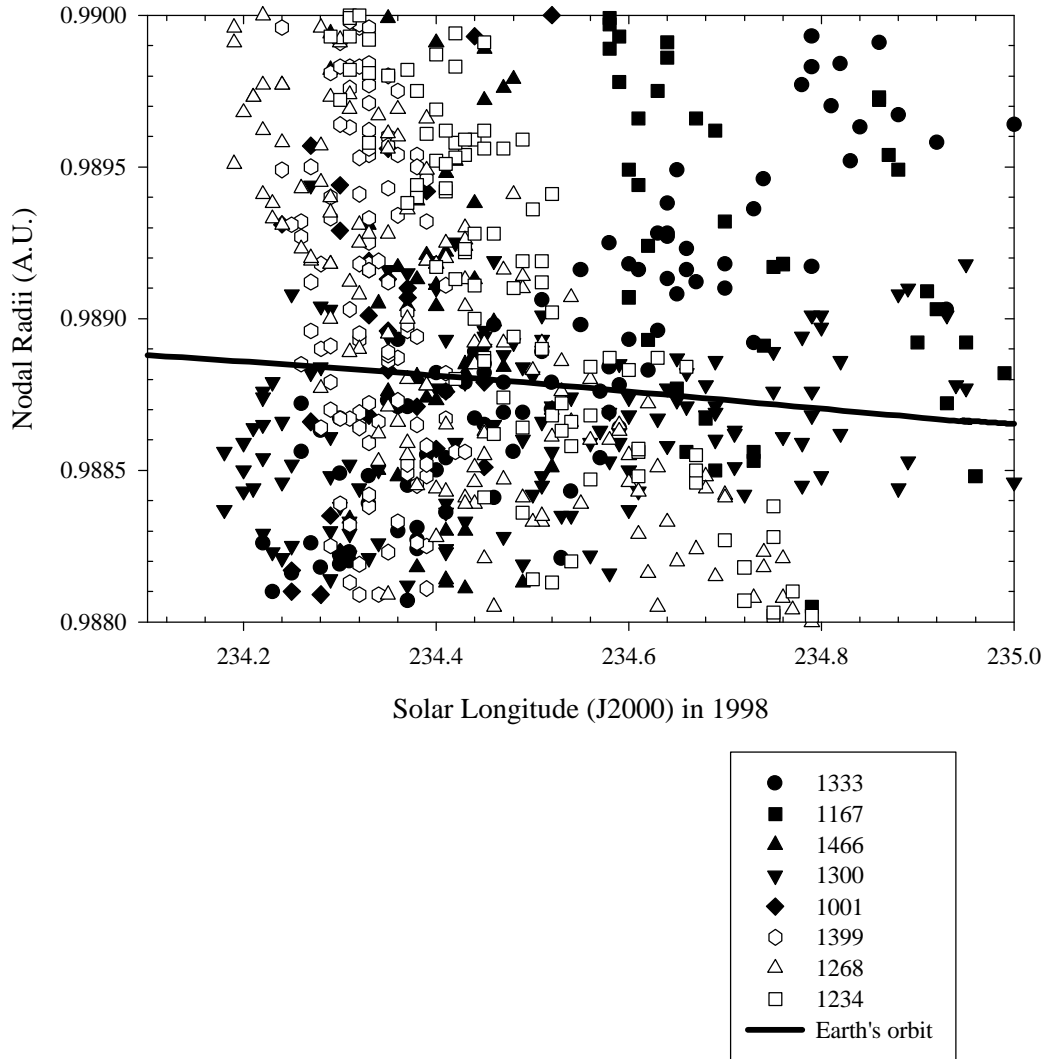


Figure 4. Nodal radii and longitudes for meteoroids ejected at different epochs (see legend) of mass 10g and density 0.8 gcm^{-3} .

To decipher further the likely dynamical cause of the nodal peak, we examined the few particles accepted as possible 1998 Leonids from these three ejection intervals. Of the 840000 test particles ejected at each perihelion from all 12 models, a total of 0, 15 and 9 test particles ended up within 0.001 A.U. of Earth's orbit and passed through their descending node within one week of the Earth in 1998 from ejections in 1899, 1932 and 1965 respectively. For these test particles, the ensemble from 1932 had a mean solar longitude at the descending node of $\lambda=235.^{\circ}22 \pm 0.^{\circ}07$. while those from 1965 were located at $\lambda=235.^{\circ}34 \pm 0.^{\circ}04$. This immediately suggests a possible linkage of the first flux peak (located at $\lambda=235.^{\circ}21$) with 1932 material and the second flux peak located at $\lambda=235.^{\circ}33$ with 1965 ejecta. Several ejection origins for this material in 1998 from the simulations are evident. For the 1965 ejecta (associated with the later nodal flux peak), all associated test meteoroids had relatively large values of β , between $10^{-3} - 9 \times 10^{-3}$, with the majority of test particles near 0.004-0.005. Of note, is that all accepted Leonids from the 1965 ejection were ejected post-perihelion at a distance of 2.5-4 A.U. from the sun. The required ejection velocities to make these particles into 1998 Leonids were between 20-60 ms^{-1} , with a large positive (i.e. in the direction of the comet's motion) velocity component. The exact ejection velocities, location and associated β were found to be the determining factors as to whether particles ended up with descending nodal radii near the Earth's orbit at the time of the 1998 shower.

In contrast, the action of planetary perturbations was found to be negligible to the delivery of these test meteoroids to nodal distances near Earth's orbit (and at the proper nodal passage time). For the ejecta from 1932, at least three distinct ejection origins are possible in 1998 for delivery near the nodal peak. First, a similar situation as with 1965 ejection is evident, namely particles ejected at large post-perihelion distances (more than 3 A.U.), with values of $\beta = 5 \times 10^{-3}$. As well several particles with very small $\beta = 5 \times 10^{-5}$ were found to have intersection conditions with Earth in 1998 near later solar longitudes if ejected at almost 4 A.U. pre-perihelion with low-velocities (of order 5 ms^{-1} , entirely in the direction of 55P/Tempel-Tuttle's motion. Additionally, a third population ejected just after perihelion (near 1 A.U.) at extremely high velocities (150 ms^{-1} such that the positive transverse velocity component is approximately 80 ms^{-1}) with very large $\beta=0.02$ also make it to Earth-crossing at the time of the 1998 Leonids. As with 1965 ejecta, it was found that planetary perturbations were not significant for delivery, rather radiation

pressure forces and initial ejection conditions controlled evolution to Earth-crossing at the time of the 1998 shower.

To confirm that our results are not simply the product of our initial choice of ejection velocity distribution, we re-ran the ejection simulations from 1200 - 1500 A.D. for large meteoroids (with $\beta=0$) and randomly chose ejection velocities between 0 - 20 ms^{-1} inside 2 A.U. Our results mirrored the earlier larger scale integrations; the 4 ejections between 1267-1367 A.D. being the most prolific contributors to the activity in 1998, with average solar longitudes for these particles in 1998 near $\lambda=234.^{\circ}50$ and probable ejection velocities from 5-20 ms^{-1} . From our earlier results (cf. Fig. 5), ejections outside this period also contribute particles both before and after this solar longitude interval, providing a plausible explanation for the observed long duration of the broad, large mass Leonid component.

We further note that the population of particles from all of these ejections had average osculating semi-major axis values at their descending nodal passages of 10.36-10.38 A.U., with very small dispersion in these averages. This is near the average semi-major axis of 10.35 A.U. value for the 5:14 resonance (Asher et al. 1999), further confirming this mechanism as the probable cause of the large particle population in 1998. We also compared these revised integrations to the observational results of Betlem et al. (1999). In particular we have found that adding ejection epochs other than 1333 broadens the final orbital distribution of particles responsible for the fireball peak. In particular, using only the results of the ejections from 1000 - 1500 A.D. we find a spread in inclinations from $161.^{\circ}7-162.^{\circ}2$ and in the argument of perihelion from $171.^{\circ}5-172.^{\circ}$. As noted in Betlem et al. (1999) the observed orbital distribution from photographic data gathered during the fireball maximum on Nov 16/17 shows ranges in these elements of $161.^{\circ}6-162.^{\circ}4$ and $169.^{\circ}5-172.^{\circ}$ respectively. Inclusion of test particles of many differing ages improves the fit between the observed and theoretical spreads (notably in the inclination distribution) in these orbital elements when compared to the single return spread which assumes 1333 as the sole source of the fireball material from Asher et al. (1999). However, some discrepancy (particularly in the argument of perihelion) between our resulting modelled distributions and those observed remains.

From the original data given in Betlem et al. (1999), however, all but a handful (4) of the observed Leonids with arguments of perihelion much smaller than the

theoretical range have large enough error in ω to overlap our final modelled range in this quantity. From the visually determined flux, we have resolved the nodal "peak" into two distinct peaks, centred at $\lambda=235.^{\circ}21 \pm 0.^{\circ}02$ and a second maximum at $\lambda=235.^{\circ}33 \pm 0.^{\circ}01$. Jenniskens (1999) examined video flux data in this interval and noted an unusual asymmetric shape to the flux profile (which he found to peak at $\lambda=235.^{\circ}31 \pm 0.^{\circ}01$). He suggests that this broad asymmetric peak is caused by contributions from two distinct (but in his data unresolved) ejections of recent origins. We find a very similar picture, with the flux profile clearly showing the locations of two distinct peaks and are able to match tentatively these from modelling with ejecta from 1932 (for the earlier sub-maxima) and 1965 (from the later sub-maxima) based on the solar longitudes of resulting test particles from those epochs. Additionally, we have found the test particles from 1932 and 1965 to have several possible ejection origins/physical characteristics. All were (generally) found to be high- β meteoroids (from 0.005-0.02) and the ejecta from 1965 appears to be associated potentially with more distant post-perihelion activity ($r > 2.5$ A.U.) with high ejection velocities. The earlier peak (from 1932 ejecta) was also found to have some test particles with a similar ejection origin as those from 1965. But, in addition to these, some test particles were found to be very high β particles ejected with exceptionally large velocities (of order 150 ms^{-1}) near perihelion and large meteoroids (with small β) ejected at large distance pre-perihelion. While any/all of these origins are possible, it is notable that the origins with high velocity, particularly distant ejections (as well as near perihelion for 1932, for example) also cause a large spread in the resulting orbital elements.

Indeed, Betlem et al. (1999) remark that the large dispersion in orbital elements from Leonids recorded on the night of Nov 17/18, 1998 (during the nodal peak) may be ascribed to ejection velocities of order 100 ms^{-1} (assuming an origin 2-4 revolutions in age). This is qualitatively consistent with our findings from modelling and we suggest by implication that the material associated with the nodal peak in 1998 comprised the "tail" of the high velocity, high β , meteoroids released by 55P/Tempel-Tuttle in 1932 and 1965. This picture is also consistent with the relatively weak increase in rates observed near the nodal peak owing to the small number of particles we would expect to meet this condition as well as the lack of larger Leonids. While the majority of meteoroids released from Tempel-Tuttle (even near perihelion) would be expected to have ejection velocities 10

ms^{-1} (also based on the widths of past observed Leonids storms from Brown (1999)), unusually shaped objects might well have ejection velocities an order of magnitude greater than the average as Gustafson (1997) has emphasized.

Bibliography

- Arlt, R. 1999., Meteoroids 1998, eds. W.J. Baggaley & V. Porubcan, Astronomical Institute of the Slovak Academy of Sciences, p. 127
- Arlt, R. 1998, WGN JIMO, 26, 239
- Asher, D.J., Bailey, M.J., Emel'Yanenko, V.V. 1999, MNRAS, 307, 919
- Betlem, H. Jenniskens, P., Leven, J., ter Kuile, C., Johannik, C., Zhao, H., Chenming, L., Guanyou, L., Hu, J., Evens, S., and Spurny, P. 1999, MAPS, 34, 979
- Brown, P., Rendtel, J. 1996, Icarus, 124, 414
- Brown, P., Jones, J. 1998, Icarus, 133, 36
- Brown, P. 1999, Icarus, 138, 287
- Crifo, J.F. 1995, ApJ, 445, 470
- Gustafson, B.A.S. 1994, Rev. Planet. Space. Sci.
- Jenniskens, P. 1999. MAPS, 34, 959
- Jones, J. 1985, MNRAS, 217, 523
- Jones, J. 1995, MNRAS, 275, 773
- Mason, J. 1995, JBAA, 105, 219
- Rendtel, J., Arlt, R., and McBeath, A. 1995., Handbook for Visual Meteor Observers, (IMO), Potsdam, Germany
- Yeomans, D. 1981, Icarus, 47, 492
- Yeomans, D., Yau, K.K., Weissman, P.R, 1996, Icarus, 124, 407